ACS SENSORS

pubs.acs.org/acssensors

Article

Bright and High-Performance Genetically Encoded Ca^{2+} Indicator Based on mNeonGreen Fluorescent Protein

Landon Zarowny, Abhi Aggarwal, Virginia M. S. Rutten, Ilya Kolb, The GENIE Project, Ronak Patel, Hsin-Yi Huang, Yu-Fen Chang, Tiffany Phan, Richard Kanyo, Misha B. Ahrens, W. Ted Allison, Kaspar Podgorski, and Robert E. Campbell*

Cite This: *ACS Sens.* 2020, 5, 1959–1968

Read Online

ACCESS | Metrics & More | Article Recommendations | Supporting Information

ABSTRACT: Genetically encodable calcium ion (Ca^{2+}) indicators (GECIs) based on green fluorescent proteins (GFP) are powerful tools for imaging of cell signaling and neural activity in model organisms. Following almost 2 decades of steady improvements in the *Aequorea victoria* GFP-based GCaMP series of GECIs, the performance of the most recent generation (i.e., jGCaMP7) may have reached its practical limit due to the inherent properties of GFP. In an effort to sustain the steady progression toward ever-improved GECIs, we undertook the development of a new GECI based on the bright monomeric GFP, mNeonGreen (mNG). The resulting indicator, mNG-GECO1, is 60% brighter than GCaMP6s in vitro and provides comparable performance as demonstrated by imaging Ca^{2+} dynamics in cultured cells, primary neurons, and in vivo in larval zebrafish. These results suggest that mNG-GECO1 is a promising next-generation GECI that could inherit the mantle of GCaMP and allow the steady improvement of GECIs to continue for generations to come.

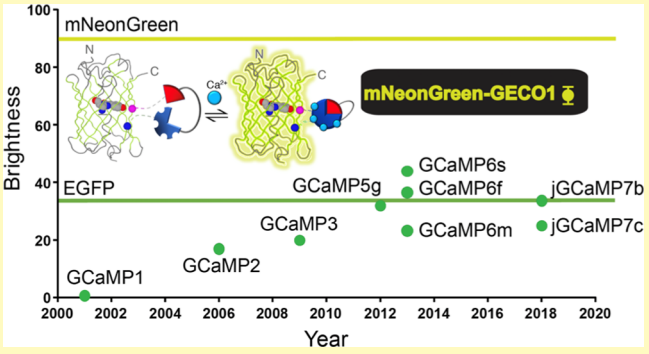

KEYWORDS: *genetically encoded biosensor, fluorescence imaging, mNeonGreen, calcium ion, neural activity imaging, GECI*

Genetically encodable calcium ion (Ca^{2+}) indicators (GECIs) are a class of single fluorescent protein (FP)-based biosensors that are powerful tools for the visualization of Ca^{2+} concentration dynamics both in vitro and in vivo.[1−3] As they are genetically encoded, GECI expression can be genetically targeted to specific cell types or subcellularly localized to specific organelles. Furthermore, their negligible cellular toxicity, minimal perturbation of endogenous cellular functions, and biological turnover make them ideal for long-term imaging experiments.[4] The Ca^{2+}-dependent fluorescent response of GECIs is routinely used as a proxy for neuronal activity due to the transient changes in Ca^{2+} concentration that accompany action potentials (AP).[5−8] GECIs have facilitated the optical recording of thousands of neurons simultaneously in the surgically exposed brains of mice.[9] Despite their widespread use by the scientific community, there are some properties of GECIs that could be further improved. These properties include faster Ca^{2+} response kinetics, higher fluorescent molecular brightness, and minimized contribution to Ca^{2+} buffering. Some GECIs have shown aggregation in neurons, and some of the most highly optimized GECIs have been demonstrated to cause aberrant cortical activity in murine models.[10−12]

An important issue that is common to all GECIs is their intrinsic Ca^{2+} buffering capacity. The Ca^{2+} binding domains of GECIs [calmodulin (CaM) or troponin C (TnC)] act as Ca^{2+} buffers within the cell and must necessarily compete with endogenous proteins for binding to Ca^{2+} (refs[13−16]). Comprehensive investigations of this phenomenon are limited, but a few reports have indicated abnormal morphology and behavior of neurons after long term or high expression of GCaMPs.[17] Ca^{2+} buffering and competition for CaM binding sites have been proposed as possible causes. One solution to the Ca^{2+} buffering phenomenon is to reduce the reporter protein expression, leading to a lower concentration of GECI and reduced buffering capacity. However, reduced expression requires increased intensity of excitation light to achieve an equivalent fluorescent signal, which can lead to increased phototoxicity and photobleaching. Another solution is to reduce the number of Ca^{2+} binding sites like that in the TnC-based GECIs, NTnC[18] and YTnC.[19] Unfortunately, these indicators have relatively low fluorescence response ($\Delta F/F_{min}$

Received: February 11, 2020
Accepted: June 23, 2020
Published: June 23, 2020

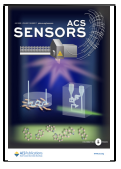

https://dx.doi.org/10.1021/acssensors.0c00279
ACS Sens. 2020, 5, 1959–1968

~ 1 for NTnC and ~10.6 for YTnC) compared to the recent jGCaMP7 variants ($\Delta F/F_{min}$ ~ 21−145).[20] Another possible solution is to develop GECIs with increased brightness such that they could be expressed at a lower concentration while retaining a similar fluorescent intensity with similar intensity of excitation light.

Further increasing the brightness of GECIs, while retaining high performance comparable to the most recent generation of indicators, would provide improved tools for optical imaging of neuronal activity and decrease the occurrence of experimental artifacts resulting from Ca^{2+} buffering and indicator overexpression.[17] Our efforts to realize this advance were inspired, in part, by the advent of a bright and monomeric engineered version of green fluorescent protein (GFP) from *Branchiostoma lanceolatum*, mNeonGreen (mNG).[21] Because of its high brightness and its excellent performance as a subcellular localization tag,[21] mNG is an exceptionally promising starting point from which to develop a brighter GECI.

Here, we introduce an mNG-based genetically encodable Ca^{2+} indicator for optical imaging (mNG-GECO1) that exceeds the brightness of all variants in the GCaMP series while providing performance that is comparable to the latest generation GCaMP variants. Key design differences between mNG-GECO1 and the GCaMP series include the GFP portion (mNG vs avGFP) and the protein topology (non-circularly permuted mNG vs circularly permuted avGFP).

EXPERIMENTAL SECTION

General Procedures. Synthetic DNA oligonucleotides and gBlocks were purchased from Integrated DNA Technologies. Plastic consumables, restriction endonucleases, Taq polymerase, Phusion polymerase, T4 DNA ligase, deoxynucleotides, DH10B *Escherichia coli*, pBAD/His B plasmid, pcDNA3.1(+) plasmid, bacterial protein extraction reagent (B-PER), penicillin−streptomycin, fetal bovine serum (FBS), TurboFect, Lipofectamine 2000, and GeneJet gel or plasmid purification kits were purchased from Thermo Fisher Scientific. Endotoxin-free plasmid DNA isolation kits were purchased from Qiagen (cat. 12362). Agarose, $MnCl_2{\cdot}4H_2O$, tryptone, D-glucose, ampicillin, L-arabinose, Hank's balanced salt solution (HBSS), Dulbecco's modified Eagle's medium (DMEM), TrypLE Express, and LB Lennox media were purchased from Fisher Scientific. NbActiv4 and neuron transfection media were purchased from Brain Bits.

3-(*N*-Morpholino)propanesulfonic acid (MOPS), ethylene glycol-bis(2-aminoethylether)-*N*,*N*,*N*′,*N*′-tetraacetic acid (EGTA), and nitrilotriacetic acid (NTA), were purchased from VWR. Nickel NTA immobilized metal affinity chromatography protein purification beads were purchased from G-BioSciences. Ionomycin and tricaine methanesulfonate were purchased from Millipore-Sigma. Ethidium bromide and polymerase chain reaction (PCR) machines (T100 Thermal Cycler) were purchased from BioRad. Gibson Assembly reagent was purchased from New England Biolabs (NEB). Genemorph II Random Mutagenesis kits and QuikChange mutagenesis kits were purchased from Agilent Technologies. Nunc 96-Well Polypropylene DeepWell Storage Plates (cat. 278743) and 96-well Nunc MicroWell 96-Well Optical-Bottom Plates (cat. 265301) were purchased from Thermo Fisher Scientific. Molecular weight cut off filters were purchased from Millipore-Sigma. Sequencing was completed by the Molecular Biology Services Unit at the University of Alberta.

Molecular Biology and Protein Engineering. Libraries for iterative directed evolution were created using Genemorph II Random Mutagenesis kits and NEB's Gibson Assembly reagent. Blunt-ended linear DNA fragments with random mutations were created using the Genemorph II kit according to the manufacturer's recommendations. Genemorph II PCR product was ligated using the NEB Gibson Assembly reagent into a linearized pBAD vector cut with XhoI/HindIII. Site saturation mutagenesis libraries were created using single and multi QuikChange mutagenesis kits according the manufacturers recommendations.

Plasmid libraries were used to transform DH10B *E. coli* which were then plated on ampicillin (100 μg/mL) and 1.5% agar plates with 0.02% L-arabinose and grown overnight (12−18 h) at 37 °C. Colonies were selected on the basis of fluorescence intensity, picked, and placed into 96-well DeepWell blocks containing 1.3 mL of LB Lennox media supplemented with 100 μg/mL ampicillin and 0.02% L-arabinose. The DeepWell blocks were shaken overnight at 37 °C. The next day, the blocks were centrifuged at 6000*g* for 5 min to pellet cells. Media was discarded and 30 μL of B-PER was added to each well. After shaking for 15 min, 200 μL of 10 mM EGTA in 30 mM MOPS/100 mM KCl pH 7.2 (MOPS/KCl buffer) was added to each well of the blocks before mixing briefly and being centrifuged again for 5 min at 6000*g*. The resulting lysate (90 μL) was loaded in each well of 96-well optical-bottom plates. Fluorescence intensity for each well of the plate was read with a Tecan Safire[2] microplate reader to determine the low Ca^{2+} intensity for each variant. High Ca^{2+} intensity was acquired by adding 15 μL of 100 mM Ca^{2+} in 30 mM MOPS pH 7.2 with a 60 s shake before reading. Taking the value of the high Ca^{2+} intensity divided by the low Ca^{2+} intensity gives a relative sensitivity value. Promising candidates, usually 8−10 variants from each 96-well block, were retested from the lysate in 10 mM low (EGTA chelated) and 10 mM high Ca^{2+} solution diluted in the MOPS/KCl buffer. The plasmids associated with the promising variants were sent for sequencing and used as template for the next round of directed evolution. For cultured neuron field stimulation experiments, GCaMP6s, jGCaMP7f, jGCaMP7s, jGCaMP7c, and jGCaMP7b plasmids (available on Addgene) were subcloned into a syn-⟨*GCaMP*⟩-IRES-mCherry-WPRE-pA vector.

Constructs for zebrafish transfection were created by ligating mNG-GECO1 PCR product into a Tol2 transposon backbone. In brief, PCR of mNG-GECO variants were ligated into the Tol2-HuC-H2B vector (Addgene plasmid #59530) cut with SalI/AgeI using Gibson Assembly. The ligated constructs were transformed into NEB Turbo Competent *E. coli* cells and grown in 250 μL of culture overnight at 30 °C. The next day, the culture was pelleted, and the DNA purified using endotoxin-free plasmid DNA purification protocol using EndoFree Plasmid Maxi Kit. The DNA was eluted with EF-free H_2O and verified by sequencing.

Protein Purification and In Vitro Characterization. To purify mNG, mNG-GECO variants, and GCaMP6s for in vitro characterization, the pBAD/His B plasmid containing the gene of interest was used to transform electrocompetent DH10B *E. coli*, which were then streaked on 100 μg/mL ampicillin/1.5% agar plates. After overnight incubation at 37 °C, a single colony was picked and inoculated to a 2 L flask containing 500 mL of 100 μg/mL ampicillin/0.02% L-arabinose liquid media and cultured for 24−30 h at 37 °C. The culture was then centrifuged at 6000*g* for 6 min to pellet the cells. Cells were resuspended in 30 mL of cold Tris-buffered saline (TBS, 150 mM NaCl, 50 mM Tris-HCl) pH 8.0 and lysed by sonication (QSonica Q700, amplitude 50, 1 s on, 2 s off, 3 min sonication time). All subsequent purification procedures were performed on ice. The resulting lysate was clarified of cell debris by centrifugation for 1 h at 21,000*g*, filtered through a Kimwipe into a 50 mL conical bottom tube, and incubated for 3 h with Ni-NTA resin. The resin containing the NTA-bound protein was washed with 100 mL of 20 mM imidazole TBS wash buffer and eluted with a 250 mM imidazole TBS elution buffer. The purified protein was buffer exchanged into TBS using a 10,000 Da molecular weight cut-off filter (Millipore-Sigma) through three successive washes. Absorption spectra were recorded on a Beckman−Coulter DU-800 UV−visible spectrophotometer and fluorescence spectra recorded on a Tecan Safire[2] plate reader.

Quantum yield (QY) determination for mNG-GECO variants was performed using mNG as a standard.[22] In brief, the concentration of protein was adjusted by dilution in MOPS/KCl pH 7.2 to reach an absorbance of 0.6−1.0. A dilution series with MOPS/KCl and 10 mM Ca^{2+} was then prepared with absorbances of 0.01, 0.02, 0.03, 0.04, and

https://dx.doi.org/10.1021/acssensors.0c00279
ACS Sens. 2020, 5, 1959−1968

0.05 for mNG, mNG-GECO variants, and GCaMP6s. Integration of the fluorescent peaks provides a total fluorescent emission value which was plotted against the absorbance to provide a slope. The QYs of mNG-GECO variants were determined using the published[22] QY value of mNG in a ratiometric manner: ($\Phi_{protein} = \Phi_{standard} \times (S_{protein}/S_{standard})$).

Extinction coefficients (EC) were determined using the alkaline denaturation method by measuring the absorption spectrum in MOPS/KCl pH 7.2 and 2 M NaOH. The absorbance value for the denatured GFP peak at 440 nm was divided by the previously determined EC of 44,000 M^{-1} cm^{-1} to give the concentration of protein.[22] Using Beer's law, the EC was then determined by dividing the MOPS/KCl buffered sample absorbance maximum by the calculated protein concentration.

Determination of K_d was performed as previously described.[23,24] In brief, a reciprocal dilution series was created with either 10 mM EGTA/10 mM CaEGTA ranging in free Ca^{2+} concentration of 0−0.039 mM or 10 mM NTA/10 mM Ca^{2+} NTA ranging in free Ca^{2+} concentration from 0 to 1.13 mM.[24] An equal amount of purified mNG-GECO was diluted 100× into 100 μL of buffer and the intensity plotted against free Ca^{2+} in triplicate. The data were then fit to a 4-parameter variable-slope in GraphPad Prism 7 software to determine the K_d.

Two-Photon Measurements. The two-photon measurements were performed in 39 μM free Ca^{2+} ($+Ca^{2+}$) buffer (30 mM MOPS, 10 mM CaEGTA in 100 mM KCl, pH 7.2) or 0 μM free Ca^{2+} ($-Ca^{2+}$) buffer (30 mM MOPS, 10 mM EGTA in 100 mM KCl, pH 7.2). The two-photon excitation spectra were acquired as previously described.[2] A protein solution of 2−4 μM concentration in $+Ca^{2+}$ or $-Ca^{2+}$ buffer was prepared and measured using an inverted microscope (IX81, Olympus) equipped with a 60×, 1.2 NA water immersion objective (Olympus). Two-photon excitation was obtained using an 80 MHz Ti-Sapphire laser (Chameleon Ultra II, Coherent) for spectra from 710 to 1080 nm. Fluorescence collected by the objective was passed through a short pass filter (720SP, Semrock) and a band pass filter (550BP200, Semrock) and detected by a fiber-coupled avalanche photodiode (APD) (SPCM_AQRH-14, Perkin Elmer). The obtained two-photon excitation spectra were normalized for 1 μM concentration and further used to obtain the action cross-section (AXS) spectra with fluorescein as a reference.[25]

Fluorescence correlation spectroscopy was used to obtain the two-photon molecular brightness of the protein molecule. The molecular brightness was defined by the rate of fluorescence obtained per total number of emitting molecules. Protein solutions (50−200 nM) were prepared in $+Ca^{2+}$ buffer and excited with 940 nm wavelength at various power ranging from 2 to 30 mW for 200 s. The obtained fluorescence was collected by an APD and fed to an autocorrelator (Flex03LQ, Correlator.com). The obtained autocorrelation curve was fit on a diffusion model through an inbuilt Matlab function[26] to determine the number of molecules $\langle N \rangle$ present in the focal volume. The two-photon molecular brightness (ε) at each laser power was calculated as the average rate of fluorescence $\langle F \rangle$ per emitting molecule $\langle N \rangle$, defined as $\varepsilon = \langle F \rangle / \langle N \rangle$ in kilocounts per second per molecule (kcpsm). As a function of laser power, the molecular brightness initially increases with increasing laser power, then levels off, and decreases due to photobleaching or saturation of the protein chromophore in the excitation volume. The maximum or peak brightness achieved, $\langle \varepsilon_{max} \rangle$, represents a proxy for the photostability of a fluorophore.

In Vitro Kinetics Analysis by Stopped-Flow. Rapid kinetic measurements of purified mNG-GECO1 and GCaMP6s were made using an Applied Photophysics SX-20 Stopped-flow Reaction Analyzer exciting at 488 nm with 2 nm bandwidth and collecting light at 520 nm through a 10 mm path at room temperature. In brief, 2 μM mNG-GECO1 and GCaMP6s proteins in 1 mM Ca^{2+} (30 mM MOPS, 100 mM KCl, pH 7.2) were rapidly mixed at 1:1 ratio with 50 mM EGTA (same buffer as above) at room temperature. k_{off} values were determined by fitting a single exponential dissociation curve to the signal decay using Graphpad Prism, with units of s^{-1}. For k_{on}, both proteins buffered in 30 mM MOPS, 100 mM KCl, and 50 μM EGTA were rapidly mixed at 1:1 ratio with varying concentrations of Ca^{2+} produced by reciprocal dilutions of 10 mM EGTA and 10 mM CaEGTA. The measured fluorescence change overtime was fitted using a 2-phase association curve to obtain the slow and fast observed rate constants (k_{obs}) for each free Ca^{2+} concentration. All measurements were done in triplicates, and values are reported as mean ± s.e.m. where noted.

Ca^{2+} Imaging in HeLa Cells. We followed previously reported protocols for our Ca^{2+} imaging experiments.[27] In brief, HeLa cells cultured in DMEM with 10% FBS supplemented with penicillin-G potassium salt (50 units/mL) and streptomycin sulphate (50 μg/mL) were plated on collagen-coated 35 mm glass bottom dishes. HeLa cells are transfected at 60% confluency with 1 μg of pcDNA3.1(+) harboring the variant of interest using 2 μL of TurboFect according to the manufacturer's recommendation. After overnight incubation at 37 °C with 5% CO_2, the cells were washed twice with prewarmed HBSS immediately before imaging. Imaging of transfected HeLa cells was performed on an inverted Zeiss 200M microscope with Semrock filters (excitation 470/40, emission 525/50) and captured with an OrcaFlash 4.0—C13440 (Hamamatsu). Images were acquired through a 40× (N.A. 1.3) oil immersion lens using the MetaMorph 7.8.0.0 software and an MS-2000 automated stage (Applied Scientific Instrumentation).

Ca^{2+} Imaging in Dissociated Rat Cortical Neurons. The mNG-GECO1 indicator was compared to other GECIs in a field stimulation assay.[28] Neonatal (P0) rat pups were euthanized, and their cortices were dissected and dissociated using papain (Worthington). Cells were transfected by combining 5×10^5 viable cells with 400 ng plasmid DNA and nucleofection solution electroporation cuvettes (Lonza). Electroporation was performed according to the manufacturer instructions. Cells were then plated at a density of 5×10^5 cells/well in poly-D-lysine coated 96-well plates. After 14−18 days in vitro, the culture medium was exchanged for an imaging buffer solution with a drug cocktail to inhibit synaptic transmission.[28] The field stimulation assay was performed as previously described.[4,20,28] In brief, neurons were field stimulated (1, 2, 3, 5, 10, 20, 40, and 160 pulses at 83 Hz, 1 ms, 40 V) and concurrently imaged with an electron multiplying charge-coupled device (EMCCD) camera (Andor iXon DU897-BV, 198 Hz, 4 × 4 binning, 800 × 800 μm, 1400 frames). Reference images were taken after stimulation to perform cell segmentation during analysis. Illumination was delivered by blue light (470 nm, Cairn Research Ltd; excitation: 450−490 nm; emission: 500−550 nm; dichroic: 495 nm long-pass). The illumination power density was measured to be 19 mW/mm^2 at the sample. Stimulation pulses were synchronized with the camera using data acquisition cards (National Instruments) controlled with Wavesurfer software (wavesurfer.janelia.org). Imaging was performed at room temperature. Data were analyzed using previously developed MATLAB (Mathworks) scripts.[20,28]

Ca^{2+} Imaging in Human iPSC-Derived Cardiomyocytes. Human iPSC-derived cardiomyocytes (human iPSC Cardiomyocytes—malelax2505) were purchased from Axol Bioscience. The 96-well glass-bottom plate or MatTek glass bottom dish (Ashland, MA, US) was first coated with fibronectin/gelatin (0.5%/0.1%) at 37 °C for at least 1 h. The cells were plated and cultured for 3 days in Axol's Cardiomyocyte Maintenance Medium. The cells then were ready for final observation with Tyrode's buffer. For electrical stimulations, iPSC-derived cardiomyocytes were plated on a MatTek glass bottom dish (Ashland, MA, US) at 100,000 cells/well. Electrical stimulation was done with 10 V, 10 ms duration, and 3 s internal using a myopacer (Ion optix c-pace ep). To image, an inverted microscope (DMi8, Leica) equipped with a 63× objective lens (NA 1.4) and a multiwavelength LED light source (pE-4000, CoolLED) was used. iPSC-derived cardiomyocytes were plated out as above, and then loaded with 5 μM Fluo-4-AM (Thermo Fisher Scientific) at room temperature for 10 min; the free dye was washed off by media replacement with preheated culture media, followed by imaging with iXon EMCCD (Andor) camera using 488 nm LED illumination. The GFP filter set (DS/FF02-485/20−25, T495lpxr dichroic mirror, and

https://dx.doi.org/10.1021/acssensors.0c00279
ACS Sens. 2020, 5, 1959−1968

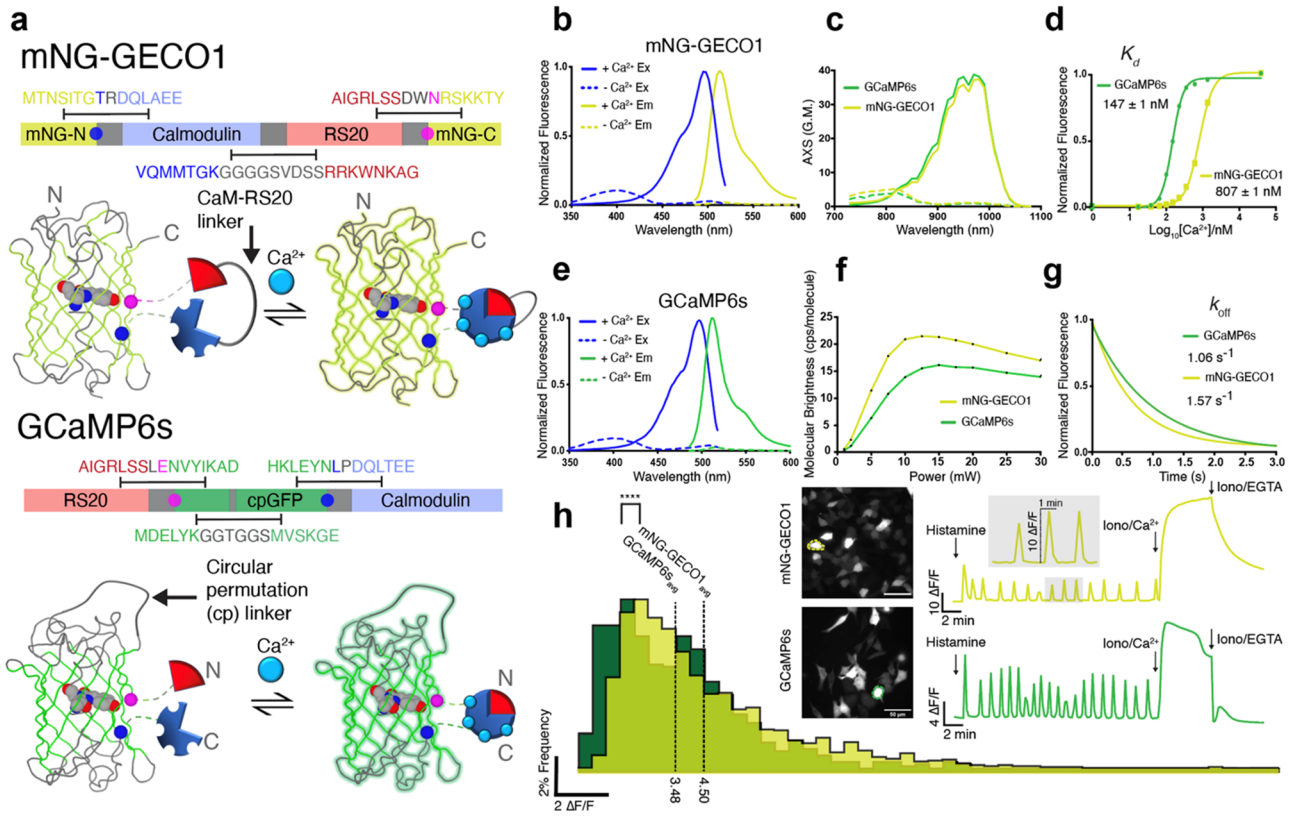

Figure 1. Topology and in vitro characterization of mNG-GECO1 and GCaMP6s. (a) Topology of non-circularly permuted mNG-GECO1 and circularly permuted GCaMP6s. Linker regions are shown in grey and the two residues that flank the insertion site (residue 136 of mNG in blue and residue 139 in magenta; numbering as in PDB ID 5LTR)[23] are shown as circles on both the protein structure and gene schematics. The Ca^{2+} responsive domains are shaded light blue for CaM and light red for RS20. (b,e) Excitation and emission spectra for each indicator. (c) Two-photon cross section for each indicator in Ca^{2+}-saturated or Ca^{2+}-free states. (d) Ca^{2+} titration for GCaMP6s (K_d = 147 ± 1 nM) and mNG-GECO1 (807 ± 1 nM). (f) Dependence of two-photon molecular brightness on excitation power intervals. (g) Stop-flow kinetics for each indicator showing mNG-GECO1 (k_{off} = 1.57 s^{-1}) and GCaMP6s (k_{off} = 1.06 s^{-1}). (h) Characterization of histamine-induced Ca^{2+} oscillations in HeLa cells with representative traces inset.

ET525/50 emission filter) was used for Fluo-4 and mNG-GECO1 observation.

Ca^{2+} Imaging in Zebrafish Larvae. To demonstrate the sensitivity and brightness of mNG-GECO1 in vivo, we performed fluorescence imaging of Ca^{2+} activity in a subset of neurons in larval zebrafish. Initially, we used the AB/WIK zebrafish strain for morphology studies (Supporting Information, Figure 4), which were treated with 1-phenol-2-thiourea to inhibit pigmentation, as described previously.[29] Later, Casper strains were available, and 20 ng/μL DNA plasmids encoding mNG-GECO1 under the control of nuclear-localized elavl3/HuC promoter (Addgene plasmid #59530) were injected into 2-cell stage embryos of Casper mutant zebrafish[24] with 40 ng/μL Tol2 transposase mRNA[30] to generate F0 transgenic zebrafish. Imaging experiments were performed using 6 day old embryos. Embryos showing expression were treated with 1 mg/mL bath-applied α-bungarotoxin (Thermo Fisher Scientific, cat. B1601) dissolved in external solution for 30 s to block movement, and subsequently incubated with 80 mM 4-aminopyridine (4AP) for 10 min. After incubation, the larvae were embedded in 2% low melting temperature agarose to prevent motion. For earlier imaging (Supporting Information, Figure 4), a Zeiss 700 confocal microscope was used with an A-Plan 10×/0.25 Ph1 M27 objective lens to obtain images of the whole larvae (Supporting Information, Figure 4a). For enlarged areas (Supporting Information, Figure 4b–e), a Plan-Apochromat 20×/0.8 M27 lens was used. Later, imaging was performed using a 488 nm laser (0.45 μM) and a 525/50 nm emission filter at 3 Hz using a Zeiss 880 confocal microscope. The laser power was set to 2.3%, gain 720, and pinhole to 29.3% open. Image acquisition, data registration, segmentation, and cell traces were handled using the Suite2p package in Python.[31] All animal procedures were approved by the Institutional Animal Care and Use Committee at the HHMI Janelia Research Campus or by the Animal Care and Use Committee: Biosciences at the University of Alberta.

RESULTS AND DISCUSSION

Rational Engineering and Iterative Directed Evolution of mNG-GECO1. We used a combination of rational design, linker sequence optimization, and directed evolution to develop mNG-GECO1 (Supporting Information, Figure 1). Starting from an unpublished topological variant of REX-GECO1,[32] we used PCR to produce a fragment containing CaM linked to the RS20 peptide with a short linker (Figure 1a). Insertion of this PCR fragment into the mNG gene between residues 136 and 137 (numbering as in PDB ID 5LTR)[33] resulted in a green fluorescent indicator prototype which we named mNG-GECO0.1 (Figure 1). For the remainder of this article, amino acids will be numbered as in the sequence alignment provided as Supporting Information, Figure 2. mNG-GECO0.1 had a minimal response to Ca^{2+} ($\Delta F/F_{min}$ = 0.3), but we anticipated that optimization of the sequence around the insertion site would yield a suitable template for directed evolution. Indeed, we found that deletion of Ala146, the residue immediately preceding the insertion of the Ca^{2+} sensing domain, substantially improved the response to Ca^{2+} (mNG-GECO0.2; $\Delta F/F_{min} \sim 2$).

https://dx.doi.org/10.1021/acssensors.0c00279
ACS Sens. 2020, 5, 1959−1968

Starting from mNG-GECO0.2, we began a process of iterative directed evolution which involved screening of libraries created from error-prone PCR or site saturation mutagenesis to identify variants with increased brightness and increased response to Ca^{2+}. In our primary library screen, we used a fluorescent colony screening system equipped with excitation and emission filters appropriate for imaging of green fluorescence.[34] Bright colonies were picked and cultured overnight in liquid media. A secondary screen for Ca^{2+} sensitivity was performed the next day using detergent-extracted bacterial lysate. The fluorescence of the lysate for each variant was measured in Ca^{2+} chelating buffer (30 mM MOPS, 100 mM KCl, 10 mM EGTA, pH 7.2) and subsequently in Ca^{2+} saturating buffer (30 mM MOPS, 100 mM KCl, 10 mM Ca^{2+}, pH 7.2). Dividing the Ca^{2+} saturated fluorescence by the Ca^{2+} free fluorescence provided an approximate but robust measure of each indicator variant's response to Ca^{2+}. For each round of screening, the plasmids were isolated for the six to ten most promising variants and sent for sequencing. The pool of these most promising variants was used as the template for the next round of library creation and directed evolution.

Following seven rounds of iterative directed evolution, *E. coli* colonies harboring mNG-GECO0.7 were brightly fluorescent after overnight incubation. However, the Ca^{2+} response of mNG-GECO0.7 remained relatively low ($\Delta F/F_{min} \sim 5$), compared to recent generation GCaMP variants. We anticipated that optimization of the linkers connecting mNG to the CaM-RS20 domain (mNG-CaM linker and RS20-mNG linker) could lead to the identification of variants with improved responses. To optimize these linker regions, we used site saturation mutagenesis to produce libraries of all 20 amino acids within the three residues connecting mNG to CaM. Individual libraries of Leu133, Thr134, and Ala135 were randomized to all 20 amino acids. If a beneficial mutation was found, the process was repeated for the remaining amino acids until these libraries were exhausted. By screening of these libraries, we identified two mutations of the linker region between mNG barrel and CaM: Ala145Gly and Leu143Ile. This variant, mNG-GECO0.9, had a $\Delta F/F_{min} \sim 12$, as measured in vitro.

Following optimization of the mNG-CaM linker, multiple site saturation libraries were created, using the same methodology as the mNG-CaM linker, for the RS20-mNG linker region (residues Glu323, Trp324, Cys325, and Arg326). Screening of these libraries led to the identification of a particularly bright variant with a Cys325Asn mutation. This variant, designated mNG-GECO0.9.1, is brighter than mNG-GECO0.9 but has a decreased response to Ca^{2+} of $\Delta F/F_{min}$ = 3.5. In an effort to improve the performance of mNG-GECO0.9.1, we applied site saturations to positions previously found to be mutated during directed evolution. Screening of these libraries for variants with increased brightness and higher $\Delta F/F_{min}$ led to the identification of a variant with Asp206Gly, Phe209Leu, Pro263Phe, Lys265Ser, Thr346Ile, and the reversion of Gly152Glu. This variant was designated as mNG-GECO1. A notable observation from the directed evolution efforts is the minimal number of mutations in the mNG domain. Only two mutations (Lys128Glu and Thr346Ile) were outside the β-strand in which the Ca^{2+} sensing domain was inserted. In contrast, three mutations were localized to the β-strand surrounding the sensing domain insertion site (Leu143Ile/Ala145Gly/Cys325Asn) and seven mutations (Thr151Ala, Thr180Cys, Asp206Gly, Phe209Leu, Pro263Phe, Lys265Ser, and Ala293Gly) were localized to the CaM domain.

In Vitro Characterization of mNG-GECO1. We characterized mNG-GECO1, in parallel with GCaMP6s, for direct comparison of biophysical properties measured under identical conditions (Supporting Information, Table 1). We found the excitation (ex) and emission (em) maxima of the Ca^{2+} saturated states to be 497 nm (ex) and 512 nm (em) for GCaMP6s and 496 nm (ex) and 513 nm (em) for mNG-GECO1 (Figure 1). The in vitro Ca^{2+} response of mNG-GECO1 ($\Delta F/F_{min}$ = 35) was similar to that of GCaMP6s when tested in parallel ($\Delta F/F_{min}$ = 39). The K_d of mNG-GECO1 (807 nM) is substantially higher than that of GCaMP6s (147 nM). mNG-GECO1 exhibits slightly faster k_{off} kinetics (k_{off} = 1.57 ± 0.01 s^{-1}) than GCaMP6s (k_{off} = 1.06 ± 0.01 s^{-1}) and similar k_{on} kinetics (Supporting Information, Figure 3).

In the Ca^{2+} bound state, mNG-GECO1 has an EC of 102,000 M^{-1} cm^{-1} and QY of 0.69, giving it an overall brightness (=EC × QY) of 70. This value is similar to the value of 77 previously reported for NTnC[18] and 78% of the brightness of mNG itself (measured by us to be 112,000 M^{-1} cm^{-1} × 0.8 = 90) (Supporting Information, Figure 4). Under two-photon excitation conditions, both mNG-GECO1 and GCaMP6s have a maximal two-photon cross section at ~970 nm and similar AXS values of 37.22 GM for mNG-GECO1 and 38.81 GM for GCaMP6s. However, because of its higher brightness at the single molecule level, the molecular brightness of mNG-GECO1 (21.3) is higher than that of GCaMP6s (16.1) at 15 mW power. Overall, these data indicate that mNG-GECO1 has excellent one-photon and two-photon excitation properties in vitro.

In Vitro Characterization in Cultured Cells and Dissociated Neurons. To compare the performance of mNG-GECO1 and GCaMP6s in cultured cells, we transfected HeLa cells with mNG-GECO1 in a pcDNA vector (CMV promoter) in parallel with pGP-CMV-GCaMP6s. Using a previously reported protocol,[27] Ca^{2+} oscillations were induced by treatment with histamine and fluorescence images were acquired every 10 s for 20 min. From the intensity versus time data for each cell, $\Delta F/F_0$ for all oscillations of $\Delta F/F_0 > 0.5$ were extracted using a Matlab script. Using these extracted $\Delta F/F_0$ values, average $\Delta F/F_0$ for all oscillations and maximum $\Delta F/F_0$ was computed. The average maximum $\Delta F/F_0$ was calculated by averaging the maximum $\Delta F/F_0$ from each responding cell. In parallel experiments, mNG-GECO1 had an average $\Delta F/F_0$ = 4.50 ± 2.96 compared to GCaMP6s's $\Delta F/F_0$ = 3.48 ± 2.40 (Figure 1h). The maximum $\Delta F/F_0$ was 16.8 ± 10.5 for mNG-GECO1 and 12.8 ± 6.11 for GCaMP6s. At the end of the 20 min imaging experiment, the cells were treated with ionomycin/Ca^{2+} to saturate the indicators and induce a fluorescent maximum and then with Ca^{2+} chelator EGTA/ionomycin to deplete Ca^{2+} and produce a fluorescent minimum. For these treatments, $\Delta F/F_{min}$ = 48.8 ± 15.1 for mNG-GECO1 and $\Delta F/F_{min}$ = 16.7 ± 5.2 for GCaMP6s. These results were obtained from a data set of 137 responding cells with 1624 individual oscillations for mNG-GECO1 and 99 responding cells with 687 individual oscillations for GCaMP6s (Supporting Information, Table 2).

We next characterized the performance of mNG-GECO1 in dissociated rat cortical neurons alongside GCaMP series indicators GCaMP6s, jGCaMP7s, jGCaMP7b, jGCaMP7c,

https://dx.doi.org/10.1021/acssensors.0c00279
ACS Sens. 2020, 5, 1959−1968

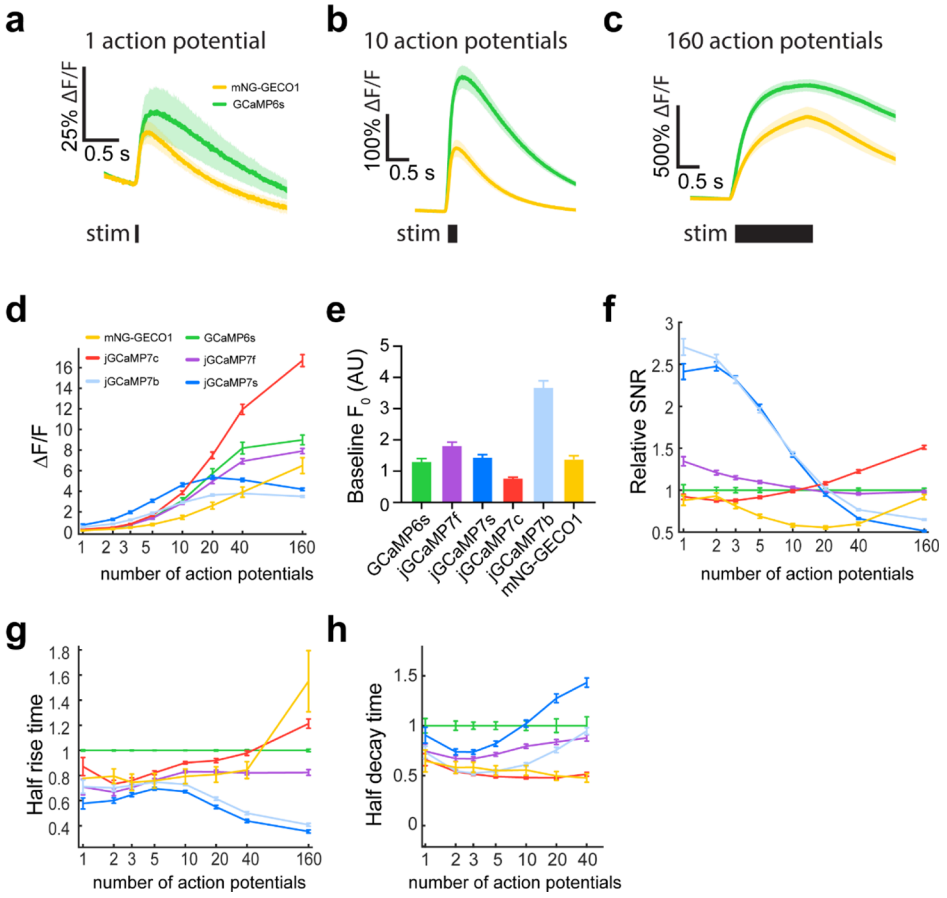

Figure 2. Characterization of mNG-GECO1 and GCaMP series indicators in dissociated rat hippocampal neurons. (a–c) Average responses to 1, 10, and 160 APs for mNG-GECO1 and GCaMP6s. Shaded areas correspond to s.e.m. for each trace. (d) Response amplitude $\Delta F/F_0$ for mNG-GECO1 and the GCaMP series of indicators in response to 1, 2, 3, 5, 10, 20, 40, and 160 APs. Data are presented normalized to $\Delta F/F_0$ of GCaMP6s. (e) Baseline brightness for each indicator, defined as the mean raw fluorescence intensity of all neurons prior to the stimulus. (f) Relative SNR, defined as the peak raw fluorescence divided by the signal standard deviation prior to the stimulus, normalized to SNR of GCaMP6s. (g) Half-rise time normalized to GCaMP6s. (h) Half-decay time normalized to GCaMP6s. The 160 AP measurement was omitted because fluorescence levels generally did not return to baseline over the imaging period. For (a–h) mNG-GECO1: 621 neurons, 15 wells; GCaMP6s: 937 neurons, 17 wells; jGCaMP7c: 2551 neurons, 44 wells; jGCaMP7b: 2339 neurons, 47 wells; jGCaMP7f: 2585 neurons, 48 wells; and jGCaMP7s: 2249 neurons, 47 wells. Data in (d–h) shown as mean ± s.e.m., see the Supporting Information, Table 3 for analyzed data.

and jGCaMP7f (Figure 2). Field-stimulated neurons expressing mNG-GECO1 had a single AP $\Delta F/F_0$ = 0.19 ± 0.04, slightly lower than that of GCaMP6s ($\Delta F/F_0$ = 0.27 ± 0.09, Figure 2a). For 10 APs, performance of mNG-GECO1 was approximately 2-fold lower than that for GCaMP6s, with $\Delta F/F_0$ of 1.5 ± 0.19 and 3.1 ± 0.26 for mNG-GECO1 and GCaMP6s, respectively (Figure 2b). At 160 APs, mNG-GECO1 has a $\Delta F/F_0$ of 6.5 ± 0.8, slightly lower than GCaMP6s's $\Delta F/F_0$ of 9.0 ± 0.47 (Figure 2c). The baseline brightness of mNG-GECO1 (1374 ± 31 AU) was comparable to the baseline brightness of GCaMP6s (1302 ± 6 AU) and jGCaMP7s (1397 ± 11 AU) (Figure 2e). The signal-to-noise ratio (SNR) of mNG-GECO1 and GCaMP6s are comparable for one and three APs (Figure 2f). For three AP stimulations, mNG-GECO1 exhibited a half-rise time of 49 ± 1 ms and half-decay time of 582 ± 12 ms. Under the same conditions, GCaMP6s exhibited a half-rise time of 65 ± 2 ms and a half-decay time of 1000 ± 36 ms. Field-stimulated neuron data is summarized in the Supporting Information, Table 3. The overall data in cultured neurons suggest that the mNG-GECO1 sensor is comparable in signal, kinetics, and baseline brightness to the GCaMP6s sensor.

In Vivo Evaluation of mNG-GECO1. To evaluate mNG-GECO1 for in vivo expression in zebrafish neurons, we used a Tol2 transposase transgenesis system to deliver mNG-GECO1 or GCaMP6s under a pan-neuronal Elavl3 promoter into zebrafish embryos.[30] We tracked the expression of mNG-GECO1 over several days to evaluate the viability of transgenic fish (Supporting Information, Figure 5). We found no obvious morphological anomalies during the larval development stage of zebrafish expressing mNG-GECO1 or GCaMP6s.

To evaluate the relative performance of mNG-GECO1 and GCaMP6s for imaging of neuronal activity in zebrafish larvae, we used the same transgenesis protocol to produce Casper zebrafish lines expressing each indicator (Figure 3). Prior to imaging, 5–6 days post-fertilization Casper fish expressing the sensors were immobilized with bungarotoxin (1 mg/mL) for 30 s followed by a 10 min incubation in the convulsant 80 mM 4-AP. The fish were then placed in low melting agar and immersed in a solution of 4-AP (80 mM). Imaging consisted of 5 min intervals of the hindbrain or midbrain at a recording rate of 3 Hz. For each indicator, five fish were imaged under six different fields of view (FOV) resulting in 834 and 1280 individual cells for mNG-GECO1 and GCaMP6s, respectively

https://dx.doi.org/10.1021/acssensors.0c00279
ACS Sens. 2020, 5, 1959–1968

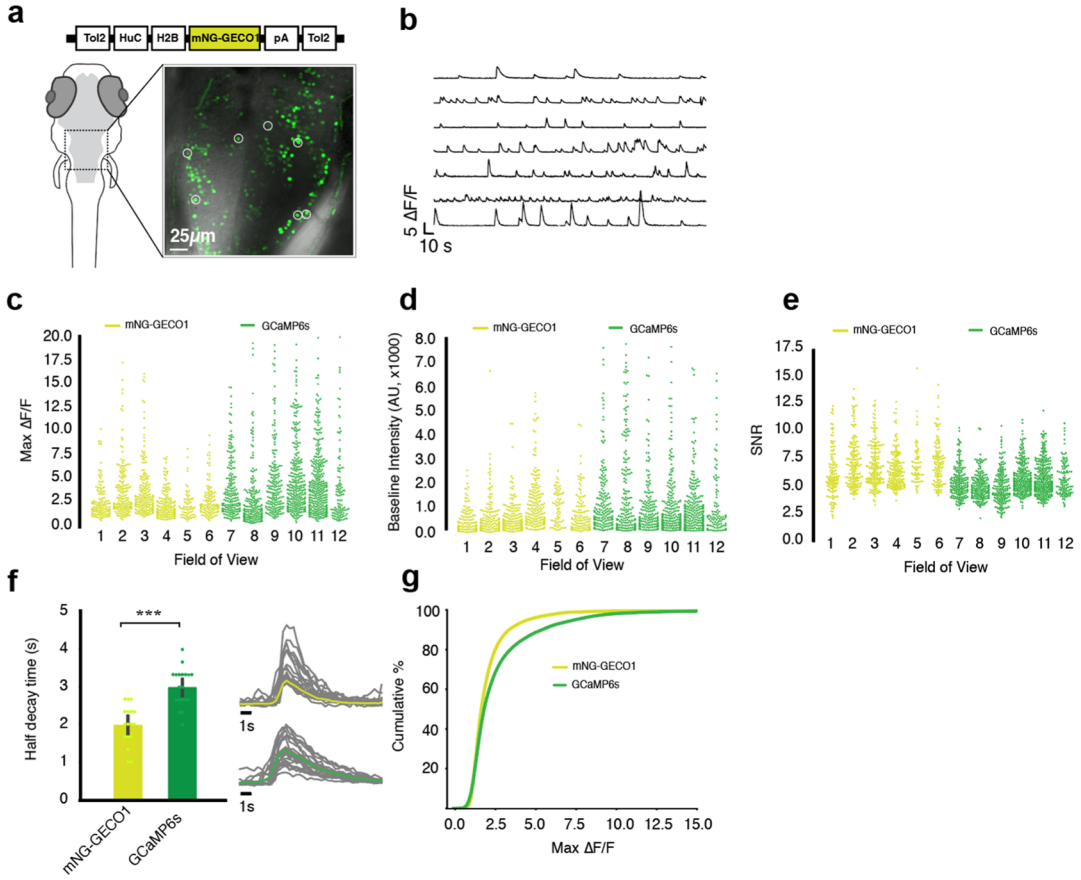

Figure 3. Characterization of mNG-GECO1 and GCaMP6s in transgenic zebrafish hind brain tissue. (a) Schematic representation of Tol2[HuC-H2B-mNG-GECO1] construct and confocal image of 1 fish (5−6 days post fertilization) with 7 regions of interest (ROI) circled. (b) Traces of ROI's from (a). (c) Max $\Delta F/F_0$ calculated by taking the max peak of each cell within the field of interest over 5 min; 6 ROI's each are used from 5 independent fish expressing mNG-GECO1 and 5 fish expressing GCaMP6s. (d) Baseline fluorescence intensity of each cell within all ROIs from 5 fish; confocal settings are kept consistent between GCaMP6s and mNG-GECO1 imaging. (e) SNR computed by dividing $\Delta F/F_0$ by raw standard deviation of each cell across 6 FOVs each for both sensors. (f) Average half-decay time plotted for mNG-GECO1 (n = 17) and GCaMP6s (n = 19) by averaging randomly selected peaks. (g) Cumulative distribution of mNG-GECO1 vs GCaMP6s. All cells are arranged in incremental order of $\Delta F/F_0$ and plotted with respect to their $\Delta F/F_0$ and their position in the order (%).

(Supporting Information, Figure 6). The resulting data was evaluated using the Suite2p package (github.com/MouseLand/suite2p).[31] We found that mNG-GECO1 had a maximum $\Delta F/F_0$ for each cell of 3.09 ± 0.08 compared to 4.56 ± 0.11 for GCaMP6s (Figure 3c). The baseline fluorescence of GCaMP6s was higher compared to that of mNG-GECO1 (1.41 ± 0.05 vs 0.95 ± 0.03 AU, respectively) (Figure 3d). However, the SNR, which was computed by dividing $\Delta F/F_0$ by the raw standard deviation of each cell in 6 FOV, was higher for mNG-GECO1 (SNR = 6.63 ± 0.07) than for GCaMP6s (SNR = 5.25 ± 0.04) (Figure 3e). We also found that mNG-GECO1 had a shorter decay time (faster k_{off} kinetics) compared to GCaMP6s (1.98 ± 0.12 vs 3.00 ± 0.12 s, respectively) (Figure 3f). The overall data in zebrafish neurons suggest that mNG-GECO1 is comparable in SNR, kinetics, and baseline brightness to the GCaMP6s sensor (Supporting Information, Table 4).

Ca^{2+} Imaging in Human iPSC-Derived Cardiomyocytes. Chemical Ca^{2+} dyes such as Fluo-4 acetoxymethyl (AM), Rhod-2 AM, and Fura-2 AM are often used to phenotype Ca^{2+} transients in induced pluripotent stem cell-derived cardiomyocytes. However, these dyes can be toxic[35,36] and may potentially suppress the activity of Na^+- and K^+-dependent adenosine triphosphatase.[37] As such, we tested whether mNG-GECO1 could serve as a robust tool for observing cells signaling and drug response while preventing cellular toxicity in iPSC-CMs (Supporting Information, Figure 7). We found that when iPSC-CMs expressing mNG-GECO1 or Fluo-4 AM were treated with 20 mM caffeine, mNG-GECO1 had a 2.8-fold higher $\Delta F/F$ response than Fluo-4 ($\Delta F/F$ = 11.77 ± 2.82 and 4.18 ± 1.27, respectively) (Supporting Information, Figure 7a,b). However, when cells were subjected to 0.33 Hz electrical stimulation for 30 min, mNG-GECO1 had a slightly lower peak $\Delta F/F$ (2.26 ± 0.81) than Fluo-4 AM (3.31 ± 1.42) (Supporting Information, Figure 7c,d). We suspect that this discrepancy is due to mNG-GECO1's lower affinity for Ca^{2+}. When we stimulated the cells in the presence of 20 mM caffeine, the max $\Delta F/F$ of mNG-GECO1 ($\Delta F/F$ = 14.20 ± 4.67) was higher than the max $\Delta F/F$ of Fluo-4 AM ($\Delta F/F$ = 6.73 ± 1.19) (Supporting Information, Figure 7e,f). Based on this data, we propose that mNG-GECO1 may serve as a useful tool for phenotypic screening and functional tests in iPSC-CMs.

SUMMARY

mNG-GECO1 is a new, first-generation, genetically encodable Ca^{2+} indicator that provides performance comparable to 6th and 7th generation GCaMP indicators. We have demonstrated

https://dx.doi.org/10.1021/acssensors.0c00279
ACS Sens. 2020, 5, 1959−1968

that the in vitro performance of mNG-GECO1 in cultured HeLa cells is on par or better than that of GCaMP6s. However, in vitro cultured neuron benchmarking as well as in vivo imaging in transgenic zebrafish larvae have indicated that further engineering and directed evolution efforts will be required to produce an mNG-GECO1 variant that provides substantial advantages relative to the jGCaMP7 series.

While this work was under review, Subach et al. reported NCaMP7, a high-performance mNG-based GECI with a very similar design to mNG-GECO1 (ref 38). Both mNG-GECO1 and NCaMP7 have performance that is comparable to GCaMP6s for in vivo imaging of neuronal activity, and it remains to be seen how these two indicators compare side-by-side. Based on in vitro characterization, mNG-GECO1 is the brighter of the two mNG-based GECIs (EC × QY = 70 for mNG-GECO1 and 57 for NCaMP7), whereas NCaMP7 has the larger fluorescence response ($\Delta F/F_0$ = 35 for mNG-GECO1 and 89 for NCaMP7) and higher Ca^{2+} affinity (K_d = 807 nM for mNG-GECO1 and 96 nM for NCaMP7). Together these two indicators clearly demonstrate that mNG is a versatile and promising scaffold for the development of next generation GECIs. Combining the mutations present in both GECIs, using the NCaMP7 crystal structure as a guide, is a promising approach to developing a substantially improved next-generation GECI that could potentially surpass jGCaMP7 in terms of overall performance.

In summary, we have developed a first generation GECI from the mNG scaffold that retains the high fluorescent brightness in vitro with performance comparable to the state-of-the-art GECI, GCaMP6s. We expect mNG-GECO1 to be just as amenable to further optimization as the first-generation GCaMP, and so mNG-GECO1 is likely to serve as the parent of a new and improved lineage of high-performance GECIs.

■ ASSOCIATED CONTENT

Supporting Information

The Supporting Information is available free of charge at https://pubs.acs.org/doi/10.1021/acssensors.0c00279.

In vitro characterization of mNG-GECO1 and GCaMP6s; characterization of Ca^{2+}-dependent fluorescence of mNG-GECO1 and GCaMP6s in HeLa cells; mNG-GECO1 comparison with GCaMP series sensors in dissociated rat hippocampal neurons; mNG-GECO1 comparison with GCaMP6s in larval zebrafish 6 dpf; overview of mNG-GECO1 development; sequence alignment of mNG-GECO variants; k_{on} traces of mNG-GECO1 and GCaMP6s; in vitro brightness comparison of mNG-GECO1 to GCaMP series; mNG-GECO1 expression profile in zebrafish larvae; mNG-GECO1 and GCaMP6s FOV in zebrafish larvae used for quantification; and comparison of Fluo-4 Ca^{2+} dye and mNG-GECO1 in human iPSC-derived cardiomyocytes (PDF).

■ AUTHOR INFORMATION

Corresponding Author

Robert E. Campbell − *Department of Chemistry, University of Alberta, Edmonton, Alberta T6G 2G2, Canada; Department of Chemistry, Graduate School of Science, The University of Tokyo, Tokyo 113-0033, Japan;* orcid.org/0000-0003-0604-092X; Email: robert.e.campbell@ualberta.ca

Authors

Landon Zarowny − *Department of Chemistry, University of Alberta, Edmonton, Alberta T6G 2G2, Canada*

Abhi Aggarwal − *Department of Chemistry, University of Alberta, Edmonton, Alberta T6G 2G2, Canada; Howard Hughes Medical Institute, Ashburn, Virginia 20147, United States*

Virginia M. S. Rutten − *Howard Hughes Medical Institute, Ashburn, Virginia 20147, United States; Gatsby Computational Neuroscience Unit, UCL, London WC1E 6BT, U.K.*

Ilya Kolb − *Howard Hughes Medical Institute, Ashburn, Virginia 20147, United States*

The GENIE Project

Ronak Patel − *Howard Hughes Medical Institute, Ashburn, Virginia 20147, United States*

Hsin-Yi Huang − *LumiSTAR Biotechnology, Inc., Taipei City 115, Taiwan*

Yu-Fen Chang − *LumiSTAR Biotechnology, Inc., Taipei City 115, Taiwan*

Tiffany Phan − *Department of Chemistry, University of Alberta, Edmonton, Alberta T6G 2G2, Canada*

Richard Kanyo − *Department of Biological Sciences, University of Alberta, Edmonton, Alberta T6G 2E9, Canada*

Misha B. Ahrens − *Howard Hughes Medical Institute, Ashburn, Virginia 20147, United States*

W. Ted Allison − *Department of Biological Sciences, University of Alberta, Edmonton, Alberta T6G 2E9, Canada;* orcid.org/0000-0002-8461-4864

Kaspar Podgorski − *Howard Hughes Medical Institute, Ashburn, Virginia 20147, United States*

Complete contact information is available at: https://pubs.acs.org/10.1021/acssensors.0c00279

Author Contributions

L.Z., A.A., and T.P. performed the directed evolution experiments and in vitro characterization. RP performed the in vitro two-photon characterization, I.K. and TGP conducted and analyzed the cultured neuron experiments. R.K. conducted the initial expression experiments of mNG-GECO1 and its variants in zebrafish under the supervision of W.T.A. V.M.S.R. completed the zebrafish characterization under the supervision of M.B.A. H.-Y.H. and Y.-F.C. did the experiments in human iPSC-derived cardiomyocytes. L.Z., A.A., K.P., and R.E.C. wrote and edited the manuscript. L.Z. and A.A. contributed equally to this work. All authors were allowed to review and edit the manuscript before publication.

Notes

The authors declare the following competing financial interest(s): The University of Alberta and Allele Biotechnology intend to file a patent application describing mNG-GECO1.

■ ACKNOWLEDGMENTS

We thank the University of Alberta Molecular Biology Services Unit (University of Alberta) and Molecular Bio (Janelia) for technical support. We thank Christopher Cairo (University of Alberta), Andy Holt (Alberta), and Loren Looger (Janelia) for providing access to the instrumentation and Eric Schreiter (Janelia) for providing access to resources and for useful feedback regarding the manuscript. We thank Deepika Walpia (Janelia) and the JRC Histology group for preparing cultured neurons. We thank John Macklin (Janelia) for overseeing two-photon measurements. We thank Nathan Shaner and co-

workers for the development of mNG FP. R.E.C. acknowledges the Japan Society for the Promotion of Science (JSPS), Natural Sciences and Engineering Research Council of Canada (NSERC), and Canadian Institutes of Health Research (CIHR) for funding support. The mNG gene was a kind gift from Jiwu Wang at Allele Biotechology. The GENIE (Genetically Encoded Neuronal Indicators and Effectors) Project (www.janelia.org/project-team/genie) is a team project at the Janelia Research Campus of HHMI set up to optimize the performance of fluorescent indicators for neuroscience applications. For this work, the GENIE project tested the performance of mNG-GECO1 relative to GCaMP6 and jGCaMP7 in neuron cultures with field stimulation and epifluorescence microscopy.

REFERENCES

(1) Mank, M.; Griesbeck, O. Genetically encoded calcium indicators. *Chem. Rev.* **2008**, *108*, 1550−1564.
(2) Akerboom, J.; Chen, T.-W.; Wardill, T. J.; Tian, L.; Marvin, J. S.; Mutlu, S.; Calderon, N. C.; Esposti, F.; Borghuis, B. G.; Sun, X. R.; et al. Optimization of a GCaMP Calcium Indicator for Neural Activity Imaging. *J. Neurosci.* **2012**, *32*, 13819−13840.
(3) Knöpfel, T. Genetically encoded optical indicators for the analysis of neuronal circuits. *Nat. Rev. Neurosci.* **2012**, *13*, 687−700.
(4) Chen, T.-W.; Wardill, T. J.; Sun, Y.; Pulver, S. R.; Renninger, S. L.; Baohan, A.; Schreiter, E. R.; Kerr, R. A.; Orger, M. B.; Jayaraman, V.; et al. Ultrasensitive fluorescent proteins for imaging neuronal activity. *Nature* **2013**, *499*, 295−300.
(5) Pologruto, T. A.; Yasuda, R.; Svoboda, K. Monitoring neural activity and [Ca2+] with genetically encoded Ca2+ indicators. *J. Neurosci.* **2004**, *24*, 9572−9579.
(6) Tian, L.; Akerboom, J.; Schreiter, E. R.; Looger, L. L. Neural activity imaging with genetically encoded calcium indicators. *Prog. Brain Res.* **2012**, *196*, 79−94.
(7) Deo, C.; Lavis, L. D. Synthetic and genetically encoded fluorescent neural activity indicators. *Curr. Opin. Neurobiol.* **2018**, *50*, 101−108.
(8) Broussard, G. J.; Liang, R.; Tian, L. Monitoring activity in neural circuits with genetically encoded indicators. *Front. Mol. Neurosci.* **2014**, *7*, 97.
(9) Kim, T. H.; Zhang, Y.; Lecoq, J.; Jung, J. C.; Li, J.; Zeng, H.; Niell, C. M.; Schnitzer, M. J. Long-Term Optical Access to an Estimated One Million Neurons in the Live Mouse Cortex. *Cell Rep.* **2016**, *17*, 3385−3394.
(10) Podor, B.; Hu, Y.-l.; Ohkura, M.; Nakai, J.; Croll, R.; Fine, A. Comparison of genetically encoded calcium indicators for monitoring action potentials in mammalian brain by two-photon excitation fluorescence microscopy. *Neurophotonics* **2015**, *2*, 021014.
(11) Bootman, M. D.; Allman, S.; Rietdorf, K.; Bultynck, G. Deleterious effects of calcium indicators within cells; an inconvenient truth. *Cell Calcium* **2018**, *73*, 82−87.
(12) Steinmetz, N. A.; Buetfering, C.; Lecoq, J.; Lee, C. R.; Peters, A. J.; Jacobs, E. A. K.; Coen, P.; Ollerenshaw, D. R.; Valley, M. T.; de Vries, S. E. J.; et al. Aberrant Cortical Activity in Multiple GCaMP6-Expressing Transgenic Mouse Lines. *eNeuro* **2017**, *4*, No. ENEURO.0207.
(13) Helmchen, F.; Imoto, K.; Sakmann, B. Ca2+ buffering and action potential-evoked Ca2+ signaling in dendrites of pyramidal neurons. *Biophys. J.* **1996**, *70*, 1069−1081.
(14) Ashworth, R.; Zimprich, F.; Bolsover, S. R. Buffering intracellular calcium disrupts motoneuron development in intact zebrafish embryos. *Dev. Brain Res.* **2001**, *129*, 169−179.
(15) Briston, S. J.; Dibb, K. M.; Solaro, R. J.; Eisner, D. A.; Trafford, A. W. Balanced changes in Ca buffering by SERCA and troponin contribute to Ca handling during β-adrenergic stimulation in cardiac myocytes. *Cardiovasc. Res.* **2014**, *104*, 347−354.
(16) Timofeeva, Y.; Volynski, K. E. Calmodulin as a major calcium buffer shaping vesicular release and short-term synaptic plasticity: facilitation through buffer dislocation. *Front. Cell. Neurosci.* **2015**, *9*, 239.
(17) Yang, Y.; Liu, N.; He, Y.; Liu, Y.; Ge, L.; Zou, L.; Song, S.; Xiong, W.; Liu, X. Improved calcium sensor GCaMP-X overcomes the calcium channel perturbations induced by the calmodulin in GCaMP. *Nat. Commun.* **2018**, *9*, 1504.
(18) Barykina, N. V.; Subach, O. M.; Doronin, D. A.; Sotskov, V. P.; Roshchina, M. A.; Kunitsyna, T. A.; Malyshev, A. Y.; Smirnov, I. V.; Azieva, A. M.; Sokolov, I. S.; et al. A new design for a green calcium indicator with a smaller size and a reduced number of calcium-binding sites. *Sci. Rep.* **2016**, *6*, 34447.
(19) Barykina, N. V.; Doronin, D. A.; Subach, O. M.; Sotskov, V. P.; Plusnin, V. V.; Ivleva, O. A.; Gruzdeva, A. M.; Kunitsyna, T. A.; Ivashkina, O. I.; Lazutkin, A. A.; et al. NTnC-like genetically encoded calcium indicator with a positive and enhanced response and fast kinetics. *Sci. Rep.* **2018**, *8*, 15233.
(20) Dana, H.; Sun, Y.; Mohar, B.; Hulse, B. K.; Kerlin, A. M.; Hasseman, J. P.; Tsegaye, G.; Tsang, A.; Wong, A.; Patel, R.; et al. High-performance calcium sensors for imaging activity in neuronal populations and microcompartments. *Nat. Methods* **2019**, *16*, 649−657.
(21) Shaner, N. C.; Lambert, G. G.; Chammas, A.; Ni, Y.; Cranfill, P. J.; Baird, M. A.; Sell, B. R.; Allen, J. R.; Day, R. N.; Israelsson, M.; et al. A bright monomeric green fluorescent protein derived from Branchiostoma lanceolatum. *Nat. Methods* **2013**, *10*, 407−409.
(22) Cranfill, P. J.; Sell, B. R.; Baird, M. A.; Allen, J. R.; Lavagnino, Z.; de Gruiter, H. M.; Kremers, G.-J.; Ustione, A.; Piston, D. W.; Piston, D. W. Quantitative assessment of fluorescent proteins. *Nat. Methods* **2016**, *13*, 557−562.
(23) Tsien, R.; Pozzan, T. Measurement of cytosolic free Ca2+ with quin2. *Methods in Enzymology*; Academic Press, 1989; Vol. *172*, pp 230−262.
(24) Dweck, D.; Reyes-Alfonso, A.; Potter, J. D. Expanding the range of free calcium regulation in biological solutions. *Anal. Biochem.* **2005**, *347*, 303−315.
(25) Xu, C.; Webb, W. W. Measurement of two-photon excitation cross sections of molecular fluorophores with data from 690 to 1050 nm. *J. Opt. Soc. Am. B* **1996**, *13*, 481−491.
(26) Mütze, J.; Iyer, V.; Macklin, J. J.; Colonell, J.; Karsh, B.; Petrášek, Z.; Schwille, P.; Looger, L. L.; Lavis, L. D.; Harris, T. D. Excitation Spectra and Brightness Optimization of Two-Photon Excited Probes. *Biophys. J.* **2012**, *102*, 934−944.
(27) Palmer, A. E.; Tsien, R. Y. Measuring calcium signaling using genetically targetable fluorescent indicators. *Nat. Protoc.* **2006**, *1*, 1057−1065.
(28) Wardill, T. J.; Chen, T.-W.; Schreiter, E. R.; Hasseman, J. P.; Tsegaye, G.; Fosque, B. F.; Behnam, R.; Shields, B. C.; Ramirez, M.; Kimmel, B. E.; et al. A Neuron-Based Screening Platform for Optimizing Genetically-Encoded Calcium Indicators. *PLoS One* **2013**, *8*, No. e77728.
(29) Thorn, R. J.; Clift, D. E.; Ojo, O.; Colwill, R. M.; Creton, R. The loss and recovery of vertebrate vision examined in microplates. *PLoS One* **2017**, *12*, No. e0183414.
(30) Kawakami, K.; Takeda, H.; Kawakami, N.; Kobayashi, M.; Matsuda, N.; Mishina, M. A Transposon-Mediated Gene Trap Approach Identifies Developmentally Regulated Genes in Zebrafish. *Dev. Cell* **2004**, *7*, 133−144.
(31) Pachitariu, M.; Stringer, C.; Dipoppa, M.; Schröder, S.; Rossi, L. F.; Dalgleish, H.; Carandini, M.; Harris, K. D. Suite2p: beyond 10,000 neurons with standard two-photon microscopy. *bioRxiv* **2017**, 061507.
(32) Wu, J.; Abdelfattah, A. S.; Miraucourt, L. S.; Kutsarova, E.; Ruangkittisakul, A.; Zhou, H.; Ballanyi, K.; Wicks, G.; Drobizhev, M.; Rebane, A.; et al. A long Stokes shift red fluorescent Ca2+ indicator protein for two-photon and ratiometric imaging. *Nat. Commun.* **2014**, *5*, 5262.

https://dx.doi.org/10.1021/acssensors.0c00279
ACS Sens. 2020, 5, 1959−1968

(33) Clavel, D.; Gotthard, G.; von Stetten, D.; De Sanctis, D.; Pasquier, H.; Lambert, G. G.; Shaner, N. C.; Royant, A. Structural analysis of the bright monomeric yellow-green fluorescent protein mNeonGreen obtained by directed evolution. *Acta Crystallogr., Sect. D: Struct. Biol.* **2016**, *72*, 1298−1307.
(34) Ai, H.-w.; Baird, M. A.; Shen, Y.; Davidson, M. W.; Campbell, R. E. Engineering and characterizing monomeric fluorescent proteins for live-cell imaging applications. *Nat. Protoc.* **2014**, *9*, 910−928.
(35) Shinnawi, R.; Huber, I.; Maizels, L.; Shaheen, N.; Gepstein, A.; Arbel, G.; Tijsen, A. J.; Gepstein, L. Monitoring Human-Induced Pluripotent Stem Cell-Derived Cardiomyocytes with Genetically Encoded Calcium and Voltage Fluorescent Reporters. *Stem Cell Rep.* **2015**, *5*, 582−596.
(36) Chang, Y.-F.; Broyles, C. N.; Brook, F. A.; Davies, M. J.; Turtle, C. W.; Nagai, T.; Daniels, M. J. Non-invasive phenotyping and drug testing in single cardiomyocytes or beta-cells by calcium imaging and optogenetics. *PLoS One* **2017**, *12*, No. e0174181.
(37) Smith, N. A.; Kress, B. T.; Lu, Y.; Chandler-Militello, D.; Benraiss, A.; Nedergaard, M. Fluorescent Ca2+ indicators directly inhibit the Na,K-ATPase and disrupt cellular functions. *Sci. Signaling* **2018**, *11*, No. eaal2039.
(38) Subach, O. M.; Sotskov, V. P.; Plusnin, V. V.; Gruzdeva, A. M.; Barykina, N. V.; Ivashkina, O. I.; Anokhin, K. V.; Nikolaeva, A. Y.; Korzhenevskiy, D. A.; Vlaskina, A. V.; et al. Novel Genetically Encoded Bright Positive Calcium Indicator NCaMP7 Based on the mNeonGreen Fluorescent Protein. *Int. J. Mol. Sci.* **2020**, *21*, 1644.

https://dx.doi.org/10.1021/acssensors.0c00279
ACS Sens. 2020, 5, 1959−1968